Flame chemistry of alkane-rich gasoline fuels and a surrogate using photoionization mass spectrometry: I. Primary reference fuel

H. Selim[1,*] , A. Lucassen[2,3], N. Hansen[2], and S.M. Sarathy[1]
[1]Clean Combustion Research Center, King Abdullah University of Science and Technology (KAUST), Thuwal, Saudi Arabia
[2]Combustion Research Facility, Sandia National Laboratories, Livermore, CA94551, USA
[3]Current: Department for Thermophysical Quantities, Physikalisch Technische Bundesanstalt (PTB), 38116 Braunschweig, Germany

Abstract
Improving the gasoline engines performance requires thorough understanding of their fundamental chemistry of combustion. Since the actual gasoline fuels are difficult to examine, due to the lack of knowledge about their exact composition as well as their numerous fuel components, the approach of using simpler gasoline fuels with limited number of components or using surrogate fuels has become more common. In this study, the combustion chemistry of laminar premixed flame of different gasoline fuels/surrogate has been examined. In this particular paper, the primary reference fuel, PRF84, has been examined at equivalence ratio of 1 and pressure of 20 Torr. The gas analysis was conducted using vacuum ultraviolet photoionization mass spectrometry.

Introduction

In order to enhance the performance of reciprocating engines, jet engines, or any other equipment where chemical-to-thermal energy transformation occurs, more sophisticated experiments along with more representative reaction mechanisms are required. Consequently, the combustion chemistry of multi-components fuels has received ample recognition in the recent years. The commercial fuels (gasoline, diesel, and kerosene) contain hundreds of compounds including additives for lubrication, knock resistance, and in case of scramjet fuels icing resistance, so it is very challenging to experimentally examine their combustion properties in fundamental research. Therefore, several approaches have been followed in order to have simpler fuels, yet representative, for the fundamental research purposes. One approach is to use a surrogate fuel [1-3] mixture with tailored physical and thermochemical properties similar, to the those of the actual fuel. Examples of these mixtures are primary reference fuels (PRF) for gasoline fuels [4], JP-8 surrogates for aviation fuels [5], and biodiesel surrogates for biodiesel fuels [6]. Another approach is to develop fuels with numerous components to be used for research purposes, such as FACE fuels [7], and to facilitate the comparison of results from different research institutes. Most of the research demonstrated using these approaches aimed to identify the basic properties of the fuels, e.g. ignition delay time [8], lift-off height [9], and heat release profiles [10]. However, the information about their flame chemistry is still incomplete. Consequently, the current reaction mechanisms are not capable of predicting the actual fuels combustion properties, e.g. fuel reactivity. With the current diagnostics a detailed analysis of reactants decay and products evolution can be achieved. In this paper we study the combustion chemistry of a laminar flame of PRF 84, which is a mixture of 84% iso-octane and 16% n-heptane and has an octane number of 84. The choice of this particular mixture is emanated from the fact that its octane number is similar to the research fuels, FACE A and FACE C; hence PRF 84 is used as a surrogate for both fuels in homogenously charged compression ignition engines(HCCI) simulations [11, 12]. These fuels are also planned to be investigated in the near future.

Experimental and Numerical Methodologies

The experiments were conducted under flame conditions of stoichiometric equivalence ratio with 50% dilution with argon; the flame chamber pressure was 20 Torr. The flame was stabilized on a McKenna burner with a 6 cm diameter. Gas sampling was conducted using a quartz probe with a 0.4 mm orifice. Speciation was achieved via single-photon ionization of the sampled gas using a vacuum ultraviolet (VUV) light provided by the Advanced Light Source at Lawrence Berkeley National Laboratory. The ionized flow was introduced to a time-of-flight mass spectrometer for analysis. Mass calibration and discrimination were determined using calibration gas with pre-known compositions. Figure 1 shows a detailed schematic of the experimental setup. The burner scans were performed at fixed ionization energy over 30 mm from the burner surface, with fine gas-sampling resolution near the burner surface and coarser resolution away from the reaction zone. The burner scans were repeated at different ionization energies from 8 eV to 16.65 eV so as to identify all the species in the reaction pool and facilitate the mole fraction calculations. The flame temperatures were calculated from the correlation between the perturbed temperature and the pressure of the first stage behind the sampling cone, typically 10^{-4} Torr order of magnitude. The proportionality constant was calculated using the temperature measured at 30 mm from the burner. Platinum/platinum-rhodium thermocouple with alumina coating has been used for temperature measurements. The experimental uncertainty has been estimated previously [13]. The

* Corresponding author: hatem.selim@kaust.edu.sa

uncertainty range of the species with well-known photoionization cross sections is 15-30%. The species with unreliable photoionization cross sections and species with overlapped ionization onset, the uncertainty can be up to a factor of 2. Due to the high perturbation near the burner surface, data within the burner surface vicinity is expected to possess high uncertainty. Subsequently, the data below 1 mm are not presented, while the all the presented results were shifted 1 mm towards the burner port. Numerical simulations were conducted and compared with the experimental results. Chemkin software [14] has been used for the simulations, while the reaction mechanism developed by Lawrence Livermore National Laboratory (LLNL) has been adopted [15].

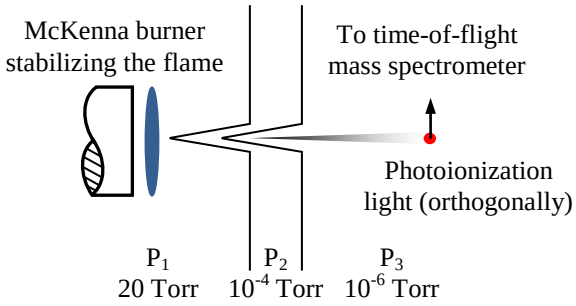

Figure 1. Schematic diagram describe the experimental setup.

Results and Discussion

A- Major Species

The mole fractions of all the presented data are calculate based on the methodology described elsewhere [16, 17]. Figure 2 describes the mole fractions of the major species in the reaction pool along with the temperature distribution against the height above the burner (HAB). Because of the low pressure of the flame chamber, the flame was about 4 to 5 mm from the burner surface; thus the peak temperatures were attained at this region. Argon mole fraction was calculated from the burner scan at 16.65 eV; hydrogen at 16.2 eV, oxygen and carbon monoxide at 14.35 eV, carbon dioxide at 15.4 eV, and water at 13.2 eV. Fuel species (C_8H_{18} and C_7H_{16}) are depleted around 3 mm, while the reaction continues for the intermediate hydrocarbon species. The major species shows monotonic trends until they reach asymptotic value. The agreement between experimental data and numerical simulations is acceptable for most of the species, except for hydrogen where some discrepancies were observed.

B- Intermediate Species

As mentioned above, fuel destruction is followed by the formation of various intermediate species, where the combustion continues to take place. In this section, presentation of selected intermediate species is provided along with the numerical simulation results.

Figure 3 shows the methane and ethane mole fractions obtained both experimentally and numerically. The mole fraction of methane was calculated from the burner scan at 14.35 eV, while ethane mole fraction was calculated from the burner scan at 12.3 eV. Both species shows very similar trend and nearly-equal peak mole fraction. The numerical predictions proved to be in good agreement with the experimental results.

The presence of oxygenated species can be initiated from different reaction pathways, mainly due to the reaction of oxygen-laden radicals with a stable species, such as, hydroxyl radical, formyl radical, peroxide radical, or methoxy radical. These reactions lead to the formation of stable oxygenated species which can be detected, e.g. ketones, enols, alcohols, and aldehydes. Figure 4 depicts the mole fraction profiles of formaldehyde and acetaldehyde in the reaction pool. Both species mole fractions were calculated at 11 eV. Formaldehyde shows one order-of-magnitude higher mole fractions than acetaldehydes. It is also expected that C_3, C_4 and higher aldehydes will have lower mole fractions. The numerical simulations successfully captures the general trend of the experimental data, however, acetaldehyde mole fraction was over-estimated by almost a factor of 2.

The utilization of the tunable photoionization source of the ALS allows the distinguishing of some of the isomers formed in the flame. For instance, the ionization energy (IE) of 1,3-butadiene ($H_2C{=}CH{-}CH{=}CH_2$) is 9.072 eV [18], while the ionization energy of 1-butyne ($HC{\equiv}C{-}CH_2{-}CH_3$) is 10.18 eV [19]. Figure 5 shows the photoionization efficiency of species m/z=54.

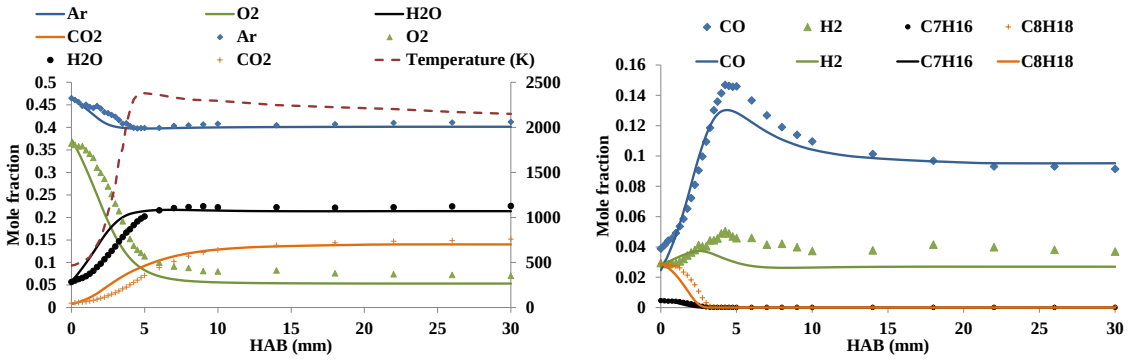

Figure 2. Mole fractions profiles of Ar, O_2, H_2O, and CO_2 (left) and CO, H_2, C_8H_{18}, and C_7H_{16} (right); experimental (symbols) and numerical (lines).

One can see that the onset of the ions formation is around 9 eV, which is attribute to 1,3-butadiene. However, the signal from 1-butyne does not appear until nearly 10.2 eV, which agrees with the previous aforementioned findings in the literature. Subsequently, the segregation of the signal of both species can be achieved by having a burner scan where the 1,3-butadiene signal exists and the 1-butyne is absent, i.e. within the 9.07 eV- 10.18 eV range. Figure 6 shows the profiles of two isomers formed in this flame, 1,3-butadiene and 1-butyne. The 1,3-butadiene mole fraction was obtained at 10 eV, while 1-butyne mole fraction was calculated at 11 eV. The reaction mechanism does not include the mole fraction of the two isomers; hence we compare the C_4H_6 mole fraction obtained from the numerical simulations with the total C_4H_6 obtained experimentally.

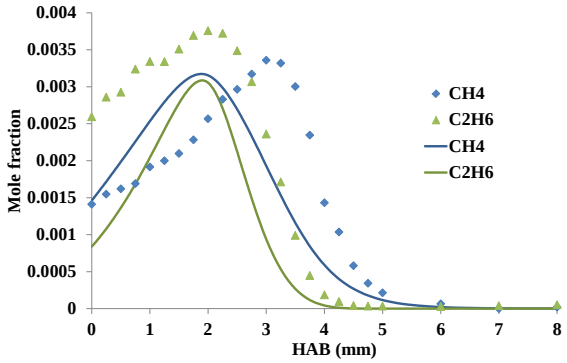

Figure 3. Mole fraction profiles for CH_4 and C_2H_6; experimental (symbols) and numerical (lines).

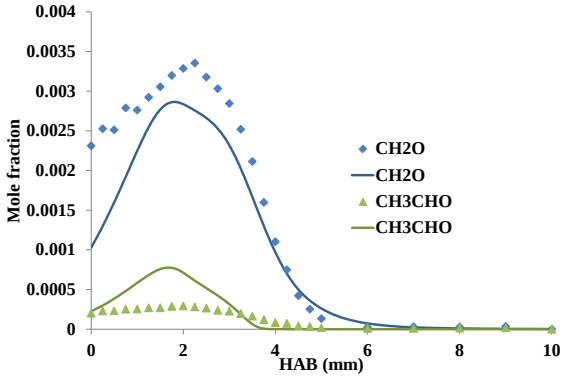

Figure 4. Mole fraction profiles of CH_2O and CH_3CHO; experimental (symbols) and numerical (lines).

Conclusions

The experiments performed in this research provide a data base about the combustion chemistry of primary reference fuel mixture, PRF84, using photoionization mass spectrometry. Single-photon ionization has been adopted using the tunable monochromatic light source available at the Advanced Light Source of Lawrence Berkeley National Laboratory. Time-of-flight mass spectrometer was used for the species analysis. Numerical simulations were conducted to compare the obtained experimental results using the reaction mechanism of Lawrence Livermore National Laboratory. The results provide comprehensive knowledge about the combustion chemistry of both fuels, which can be used for the improvement of the chemical kinetics of the available reaction mechanisms. Mole fractions of major species, selected intermediate species including alkanes, alkenes, and oxygenated species were obtained. In addition, isomeric species were distinguished using the tunable photoionization source. In general, the results showed good agreement between the experimental and numerical results. However, some discrepancies were observed, especially for the acetaldehyde profile. In addition, the reaction mechanism did not differentiate between 1,3-butadiene and 1-butyne isomers, hence the comparison was done for the total C_4H_6 mole fraction obtained experimentally with the numerical value attained for C_4H_6.

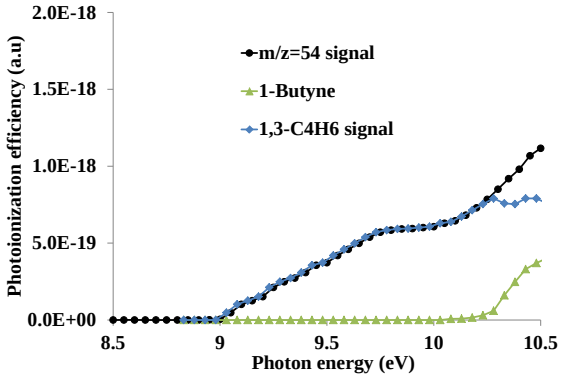

Figure 5. Mole fraction profiles for CH_2O and CH_3CHO; experimental (symbols) and numerical (lines).

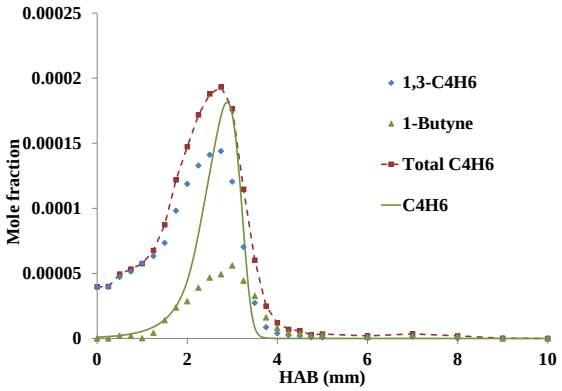

Figure 6. Mole fraction profiles for 1,3-butadiene and 1-butyne isomers; total C_4H_6 is for comparison only for comparison with numerical simulation; experimental (symbols) and numerical (lines).

Acknowledgements

The authors acknowledge funding support from the Clean Combustion Research Center and from Saudi Aramco under the FUELCOM program.
The measurements were performed within the "Flame Team" collaboration at the Advanced Light Source (ALS), Lawrence Berkeley National Laboratory, Berkeley, USA, and we thank the students and postdocs for the help with the data acquisition. The experiments at the Advanced Light Source (ALS) have profited from the expert technical assistance of Paul Fugazzi. The ALS is supported by the Director, Office of Science, Office of Basic Energy Sciences, of the U.S. Department of Energy under Contract No. DEAC02-05CH11231. Sandia is a multi-program laboratory operated by Sandia Corporation, a Lockheed Martin Company, for the National Nuclear Security Administration under contract DE-AC04-94-AL85000.

References

1. K. Anand; Y. Ra; R. Reitz; B. Bunting, Energy & Fuels 25 (4) (2011) 1474-1484
2. I. P. Androulakis; M. D. Weisel; C. S. Hsu; K. Qian; L. A. Green; J. T. Farrell; K. Nakakita, Energy & fuels 19 (1) (2005) 111-119
3. C. J. Mueller; W. J. Cannella; T. J. Bruno; B. Bunting; H. D. Dettman; J. A. Franz; M. L. Huber; M. Natarajan; W. J. Pitz; M. A. Ratcliff, Energy & Fuels 26 (6) (2012) 3284-3303
4. G. T. Kalghatgi, International Journal of Engine Research (2014) 1468087414526189
5. J. A. Cooke; M. Bellucci; M. D. Smooke; A. Gomez; A. Violi; T. Faravelli; E. Ranzi, Proceedings of the Combustion Institute 30 (1) (2005) 439-446
6. W. Liu; R. Sivaramakrishnan; M. J. Davis; S. Som; D. E. Longman; T. F. Lu, Proceedings of the Combustion Institute 34 (1) (2013) 401-409
7. T. Gallant; J. A. Franz; M. S. Alnajjar; J. M. Storey; S. A. Lewis; C. S. Sluder; W. J. Cannella; C. Fairbridge; D. Hager; H. Dettman, in: SAE Technical Paper: 2009.
8. S. S. Vasu; D. F. Davidson; R. K. Hanson, Combustion and Flame 152 (1–2) (2008) 125-143
9. O. A. Kuti; M. Sarathy; K. Nishida; W. Roberts, in: SAE Technical Paper: 2014.
10. G. Shibata; K. Oyama; T. Urushihara; T. Nakano, in: SAE Technical Paper: 2005.
11. D. Vuilleumier; H. Selim; R. Dibble; M. Sarathy, in: SAE Technical Paper: 2013.
12. M. Sjöberg; J. E. Dec, Proceedings of the combustion institute 31 (2) (2007) 2895-2902
13. F. Egolfopoulos; N. Hansen; Y. Ju; K. Kohse-Höinghaus; C. Law; F. Qi, Progress in Energy and Combustion Science (2014)
14. CHEMKIN-PRO Release 15112, San Diego, CA 92121, 2012, in.
15. M. Mehl; W. Pitz; M. Sarathy; Y. Yang; J. Dec, in: SAE Technical Paper: 2012.
16. M. Schenk; L. Leon; K. Moshammer; P. Oßwald; T. Zeuch; L. Seidel; F. Mauss; K. Kohse-Höinghaus, Combustion and Flame 160 (3) (2013) 487-503
17. T. A. Cool; K. Nakajima; C. A. Taatjes; A. McIlroy; P. R. Westmoreland; M. E. Law; A. Morel, Proceedings of the Combustion Institute 30 (1) (2005) 1681-1688
18. B. Yang; J. Wang; T. A. Cool; N. Hansen; S. Skeen; D. L. Osborn, International Journal of Mass Spectrometry 309 (2012) 118-128
19. J. Wang; B. Yang; T. A. Cool; N. Hansen; T. Kasper, International Journal of Mass Spectrometry 269 (3) (2008) 210-220